International Journal of Mass Spectrometry 279 (2009) 163–169

Contents lists available at ScienceDirect

International Journal of Mass Spectrometry

journal homepage: www.elsevier.com/locate/ijms

Isotope selective manipulation and observation of Ca^+ ions by ion trap–laser cooling technique

Y. Hashimoto*, D. Nagamoto, S. Hasegawa

Department of Quantum Engineering and Systems Science, The University of Tokyo,7-3-1 Hongo, Bunkyo-ku, Tokyo 113-8656, Japan

ARTICLE INFO

Article history:
Received 7 June 2008
Received in revised form 29 October 2008
Accepted 29 October 2008
Available online 6 November 2008

Keywords:
Ion trap
Laser cooling
Isotope manipulation
Trace isotope analysis
Calcium ion

ABSTRACT

We performed isotope selective manipulation of laser cooled ions using the mass selectivity of an ion trap. We have investigated the possibility of realizing isotope selection for even Ca^+isotopes, such as $^{40}Ca^+$ (abundance 96.9%), $^{42}Ca^+$ (0.647%), $^{44}Ca^+$ (2.09%), and $^{48}Ca^+$ (0.187%). We observed the behaviors of each isotope for the rf and dc voltages in the stable region of Mathieu equation. Even though the increase of the rf and dc voltages leads to rf heating of the trapped ions, the trapped ions were observed by the laser cooling technique. Furthermore, we demonstrated the selectivity and observation of a target isotope.

1. Introduction

Calcium is the fifth most abundant element in the earth crust, with an abundance of ∼ 3%. It is an essential element in both animal and plant tissues and has six stable isotopes, ^{40}Ca (abundance 96.9%), ^{42}Ca (0.647%), ^{43}Ca (0.135%), ^{44}Ca (2.09%), ^{46}Ca (0.004%), and ^{48}Ca (0.187%). The study of Ca isotopes is useful in many fields [1–3]. Furthermore, the analysis of ^{41}Ca ($^{41}Ca/Ca = 10^{-15} - 10^{-14}$, $t_{1/2} = 1.04 \times 10^5$ year), which is a long-lived radioactive ultra trace isotope, has applications, e.g., in biomedicine [4], archeology [5], and planetary science [6]. Today only accelerator mass spectrometry (AMS) is utilized for practical purposes because its detection limit ($\sim 10^{-15} - 10^{-13}$) is very close to the natural abundance [7]. However, this method requires a large facility and sophisticated chemical pretreatments of the samples. In order to avoid these issues, laser-based methods, such as resonance ionization mass spectrometry (RIMS) [8] and atom trap trace analysis (ATTA) [9], have been developed for laboratory application. So far, calibration of detection limits for the same samples measured by RIMS and AMS could be given in the $10^{-11} - 10^{-10}$ isotopic range [10], and for ATTA and RIMS in the $\sim 10^{-8}$ range [9].

We have an ion trap–laser cooling method for the study of the Ca isotopes. Laser cooled ions stored in an ion trap represent a nearly ideal system for atomic physics. Therefore trapped ions have promising applications in many fields, such as frequency standards [11], quantum information processing [12], isotope separation [13]. Our ultimate goal utilizes a different type of mass spectrometer and laser manipulation than RIMS and ATTA, and can be used to analyze ^{41}Ca [14]. Our method utilizes a smaller experimental system [15], and the prospect of achieving high selectivity for the target isotope by utilizing the mass selectivity of the ion trap and the isotope shift of the transition wavelength in laser cooling and repumping. Furthermore, single ions of different isotopes can be observed. For these reasons, we consider that the ion trap–laser cooling method is suitable for ultra trace isotope analysis of ^{41}Ca. Although many ion trap–laser cooling techniques have been developed, their application to ultra trace isotope analysis has not yet been realized and is not by any means a trivial problem. The abundance of ^{41}Ca is extremely low, so a special sample feeding and loading system should be required. Moreover, no one has investigated the isotope shifts of ^{41}Ca ions. Since ^{41}Ca being an odd isotope, it has nuclear spin, so the hyperfine structures of laser cooling and repumping transitions should be considered similar as for ^{43}Ca. For these reasons, it is difficult to treat ^{41}Ca from the very beginning of the research. As the first step towards realizing ultra trace isotope analysis, we constructed an ion trap–laser cooling system for $^{40}Ca^+$ ions, which have no nuclear spins [16]. As the next step, we have developed an experimental system to observe even Ca isotopes.

So far, some groups have reported isotope separation with ion trap–laser cooling methods: (a) direct cooling of the target isotope in the case of Yb^+(172(22%), 174(32%), 176(13%)) [17]; (b) utilization

* Corresponding author.
E-mail addresses: yhashi@lyman.q.t.u-tokyo.ac.jp (Y. Hashimoto), hasegawa@q.t.u-tokyo.ac.jp (S. Hasegawa).

1387-3806/$ – see front matter © 2008 Elsevier B.V. All rights reserved.
doi:10.1016/j.ijms.2008.10.021

of the nonlinear resonance in a Paul trap caused by the imperfection of the trapping potential [18,19]; (c) excitation of the secular motion by a perturbating rf field [20]; (d) selective heating and cooling method: after trapping, the frequency of the cooling laser is set to blue detuning for a certain isotope, which is eliminated from ion trap by laser heating, while the other isotopes, which are red-detuned, still remain laser cooled [13,21].

The methods (b) and (d) have been applied to Ca^+ ions [13,19], however, it is difficult to effectively eliminate the dominant isotope $^{40}Ca^+$ [13,19], therefore, some groups have ionized a particular Ca isotope by means of a selective photoionization loading [22–26].

We trap Ca^+ ions in a linear Paul trap [14,16]. In the radial direction, an rf electric field ($V_{rf}\cos\Omega t$) superimposed on a dc electric field (U_{dc}) is applied to one pair of linear electrodes, while the other pair is kept to electric ground. The electric potential is approximately given as

$$\Phi(x, y, t) = (U_{dc} + V_{rf}\cos\Omega t)\frac{x^2 - y^2}{2r_0^2}, \quad (1)$$

where r_0 is the closest distance between the surface of the linear electrode and the center of the trap. The motion of a trapped ion in the $x - y$ plane is governed by the so-called Mathieu equation [27]

$$\frac{d^2x}{d\xi^2} + (a_x - 2q_x\cos 2\xi)x = 0, \quad (2)$$

$$\frac{d^2y}{d\xi^2} + (a_y - 2q_y\cos 2\xi)y = 0, \quad (3)$$

with $a = a_x = -a_y = 4eU_{dc}/mr_0^2\Omega^2$, $q = q_x = -q_y = 2eV_{rf}/mr_0^2\Omega^2$, and $\xi = \Omega t/2$, where e and m are the charge and the mass of the ion, respectively. In the case of $a = 0$, stable trapping is achieved for $0 < q < 0.92$ [27]. We can in principle separate the laser-cooled ions with a given mass number by choosing particular a and q values. However, to the best of our knowledge, no one has demonstrated this method. One reason is that the q value should be low in order to efficiently realize laser cooling and to suppress rf heating [28]. Under these conditions, the a value should be ~ 0 to achieve stable trapping. Because of the instrumental limitation it is difficult to widely scan the rf and dc voltages in the stable diagram of Mathieu equation. Furthermore, the Mathieu equation describes only the motion of a single ion and does not include the effects of a large number of ions, isotopes and a laser cooling. As compared to quadrupole mass spectrometer (QMS) [27], in our ion trap–laser cooling method, a dc voltage is applied to the cap electrodes to trap ions in the axial direction. Therefore the effect of the cap electrode and dc voltage should also be taken into account. In addition, the behavior of a particular isotope has been reported when several isotopes are simultaneously trapped. For these reasons, in order to utilize an ion trap as a mass filter the dependence of trapped ions on the trapping voltages should be investigated, before attempting to measure $^{41}Ca^+$. We can utilize the laser cooling method using isotope shifts in order to selectively observe laser-induced fluorescence (LIF) of a particular isotope.

In this article, we report isotope selective manipulation of laser-cooled Ca^+ ions using the mass selectivity of a linear Paul trap. We can investigate dependence of the trapping efficiencies for the even Ca^+ isotopes (^{40}Ca, ^{42}Ca, ^{44}Ca, ^{48}Ca) trapped with other isotopes on the rf and dc voltages, by scanning the a and q values in the stable region of the Mathieu equation. Next, we calculate the trajectories of trapped ions with SIMION, in which we can consider the actual experimental conditions, i.e., the electrode geometry, the ion temperature, and the ion position. Finally, we demonstrate isotope selection of laser-cooled Ca^+ ions in the linear Paul trap.

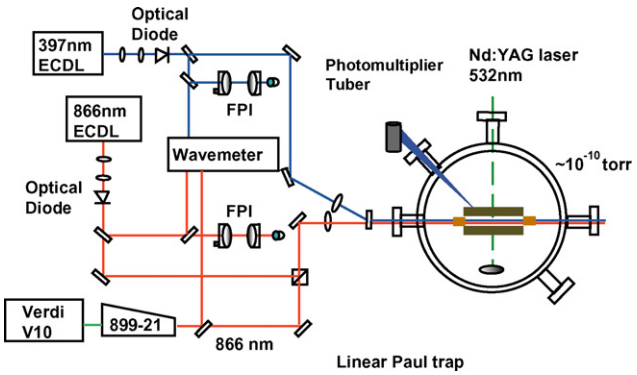

Fig. 1. Experimental setup. Our system consists of three parts: laser system: a lab-made 397 nm, Toptica made 866 nm ECDLs for laser cooling, a Nd:YBO_4 laser (Coherent Verdi V10) pumping a Ti:Sa laser (Coherent 899-21) for additional 866 nm light source, and a Nd:YAG laser for laser ablation, FPIs for stabilization of ECDLs; vacuum components: linear Paul trap, Ca target, and objective lenses; observation system: photomultiplier tube.

2. Experimental setup

The apparatus consists of a linear Paul trap in an ultra high-vacuum system (see Fig. 1), with the external cavity diode lasers (ECDLs) and a Ti:Sa laser available to drive the laser cooling and repumping transitions shown in Fig. 2. In our trap, the closest distance from the trap axis to a surface of linear electrode is approximately $r_0 = 4.3$ mm. Two end cap electrodes, of inner diameter 3 mm and outer diameter 5 mm, are positioned on the trap axis $2z_0 = 20$ mm apart. The trap electrodes are fixed in a stainless steel vacuum chamber. An rf power source supplies a trapping voltage of frequency $\Omega/2\pi = 1.5$ MHz and amplitude $V_{rf} = 35$–300 V with an offset dc voltage $U_{dc} = 0$–100 V for the linear electrodes, while two dc power supplies provide axial confining voltages $V_{cap} = 0$–35 V for the two end cap electrodes. We monitored the rf and dc voltages divided by 100 using an oscilloscope. Because of the precision of oscilloscope and the impedance change of the trap system, the error of the rf and dc voltages are ± 5 V and ± 0.2 V, respectively, which correspond to $q = \pm 0.01$ and $a = \pm 0.001$. The vacuum chamber is pumped out by a turbo molecular pump and a rotary pump. An ion gauge monitors the vacuum pressure, which is below 3.0×10^{-10} Torr, the limit of the gauge's sensitivity. To easily generate calcium ions from a solid Ca target, we utilize laser ablation with a frequency doubled Nd:YAG pulsed laser [29]. The Ca disk target, with a purity of 99.5%, is placed on a pedestal below the trap electrodes.

Fig. 2 shows the energy levels and isotope shifts of the Ca^+ isotopes [30,31]. In order to realize laser cooling and repumping, the two Littrow design ECDLs are utilized for 397 nm and 866 nm transitions, respectively. The ECDLs are locked to temperature stabilized

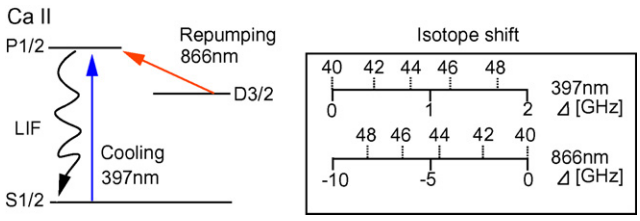

Fig. 2. Energy diagram of the Ca^+ ion. Optical transitions utilized in this experiment. Laser cooling and repumping make use of the 397 nm and 866 nm transitions, respectively. The LIF of the cooled ions is used for observing the trapped ions. Inset: the isotope shifts of the even isotopes (dotted lines, labeled with the mass number) is as a function of detuning Δ relative to $^{40}Ca^+$ [30,31].

Fabry–Perot interferometers (FPI) to reduce their linewidths below 5 MHz. In addition, the Ti:Sa laser (866 nm) is employed for the simultaneous observation of two Ca^+ isotopes because of large isotope shift of the 866 nm transition. This laser linewidth is also stabilized within 1 MHz. The beam sizes are about 1 mm. The intensities of the lasers are controlled by neutral density filters. In addition, in order to selectively observe an isotope of interest, the frequencies of the 397 nm and 866 nm lasers correspond to the isotope shifts.

The ions are detected by their LIF, which is collected in a photomultiplier tube by a designed lens system. The net detection efficiency of the system was measured to be 4×10^{-4} at 397 nm. The photon count rate observed from a single cold $^{40}Ca^+$ ion is 8 kcps [16]. The experimental data were collected, stored, and displayed by a LabVIEW-based computer system.

3. Dependence on the rf and dc voltages

3.1. Dependence on the rf voltage

In order to observe low abundance Ca^+ isotopes we should efficiently reduce the number of $^{40}Ca^+$, which is the dominant isotope. Although QMS acts in principle as a high pass filter for $U_{dc} = 0$ V [27], the effects of the cap voltage are not considered. In addition, the behavior of a particular isotope has been reported when several isotopes are simultaneously trapped. So we investigated the dependence of the ratio of $^{40,42,44,48}Ca^+$ on the rf voltage with the existence of other isotopes (Fig. 3). We can measure the behavior of an isotope of interest on the same condition except for the 397 nm and 866 nm lasers. Here, we define the ratio as $\mathrm{LIF}(V_{rf})/\mathrm{LIF}(V_{rf} = 200\,\mathrm{V})$.

When loading Ca^+, we set the trapping voltage of $U_{dc} = 0$ V, $V_{rf} = 230$ V. Here, no isotope separation is performed. After trapping, we scanned V_{rf} from 200 V to 300 V. First the number of the lightest isotope of $^{40}Ca^+$ reduces with increasing of the rf voltage. Next $^{42}Ca^+$ decreases. The volume of trapping region decreases with increasing of the rf voltage. The heavier isotopes decrease with further increasing of the rf voltage in the order corresponding to $^{44}Ca^+$ and $^{48}Ca^+$, however, $^{44}Ca^+$ and $^{48}Ca^+$ cannot be eliminated. Because the vertical axis indicates the ratio of LIF, the estimations of $^{44}Ca^+$ and $^{48}Ca^+$, which are small abundant isotopes, can be relatively large. We can also see the increasing of LIF because the cooling efficiency may be improved by the decreasing of trapped ions. Furthermore, we can consider that the effect of laser cooling for each isotope is smaller than that of the rf voltage.

Fig. 3 shows the dependence of the ratio of $^{40,42,44,48}Ca^+$ on the rf voltage since for $^{43}Ca^+$, a hyperfine pumping laser or a microwave system is required for laser cooling [25,26,32]. The natural abundance of $^{46}Ca^+$ is too small for this experimental setup. We performed the measurements at least five times under each condition considering the repeatability. The horizontal error bar results from the error of the rf amplitude. The vertical error bar is smaller than the marker size. So we can demonstrate the high pass filter function of a linear Paul trap utilizing these dependences of the ratio of Ca^+ isotopes on the rf voltage. Furthermore, we can find the dip, where the ratio drastically decreases, for each isotope.

3.2. Dependence on the dc voltage

In principle we may reduce the number of a light isotope, such as the dominant isotope of $^{40}Ca^+$, by controlling the rf voltage, while we need to control the dc voltage for the selection of a particular isotope [27]. Therefore we also investigated the dependence of ratios for each isotope on the dc voltage by scanning U_{dc} while setting the rf voltage $V_{rf} = 150$, 200, and 235 V. The conditions of loading and cooling are the same as the measurement of dependence on the rf voltage (Fig. 4). Here, we define the ratios as $\mathrm{LIF}(U_{dc})/\mathrm{LIF}(U_{dc} = 0\,\mathrm{V})$.

We can find that the order of isotope reduction changes with the rf voltage. Here, we focus the case of $V_{rf} = 150$ V in order to demonstrate the low pass filtering of trapped Ca^+ isotopes. After nonisotope selective loading of Ca^+ we scanned the dc voltage from 0 V to 40 V. First the heaviest isotope of $^{48}Ca^+$ decreases with increasing of the dc voltage, while the other isotopes can be trapped. Further increasing of the dc voltage makes the reduction of $^{44,42,40}Ca^+$ in descending order of the mass number and the remaining of lighter isotopes of $^{42}Ca^+$ and $^{40}Ca^+$ cannot be observed. This is the difference between the scanning of the rf and dc voltages.

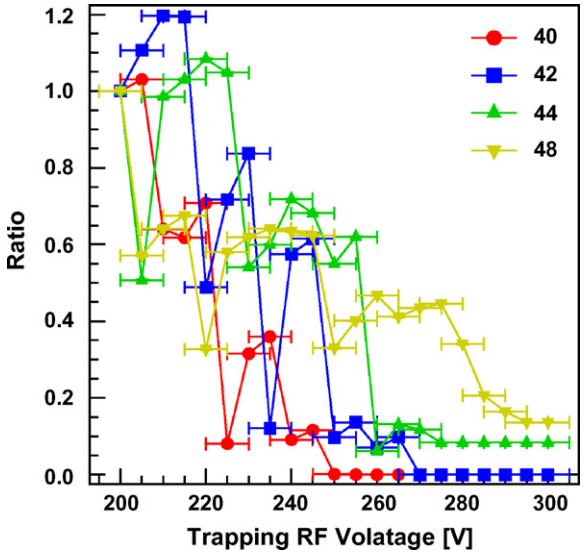

Fig. 3. Dependence of the ratio of Ca^+ isotopes on the rf voltage. The ratio is defined as $\mathrm{LIF}(V_{rf})/\mathrm{LIF}(V_{rf} = 200\,\mathrm{V})$. The trapped isotopes decrease with increasing of the rf voltage in the order corresponding to $^{40}Ca^+$, $^{42}Ca^+$, $^{44}Ca^+$, and $^{48}Ca^+$. For each isotope we can observe the dips where the ratio drastically decreases.

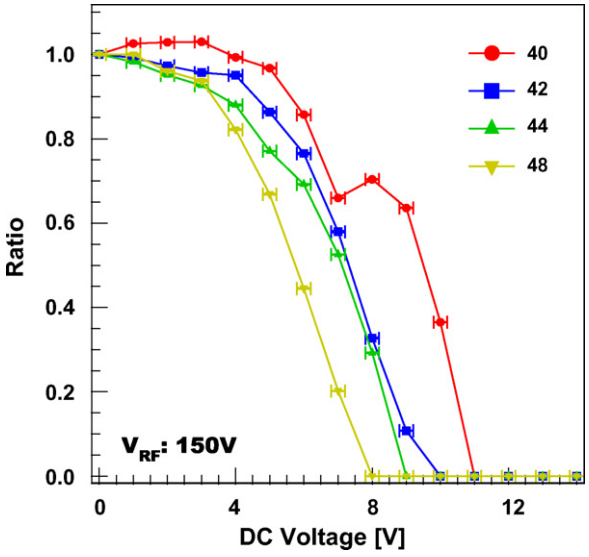

Fig. 4. Dependence of the ratio for each isotope on the dc voltage for $V_{rf} = 150$ V. The ratio monotonically decreases with increase of the dc voltage. The reduction occurs in the order of $^{48}Ca^+$, $^{44}Ca^+$, $^{42}Ca^+$, and $^{40}Ca^+$.

We performed the measurements at least five times under each condition considering the repeatability. The horizontal error bar results from the error of the dc voltage. The vertical error bar is smaller than the marker size. For each isotope the scanning range of the dc voltage is included in the stable region of the Mathieu equation, so stable trapping should be achieved in theory. However our results show the reduction of light isotope with increase of the dc voltage. $^{40}Ca^{+}$ can be trapped within the stable region in principle, however, we can consider that the background signal includes the LIF from the small number of $^{40}Ca^{+}$ because of high laser intensity. So small number of $^{40}Ca^{+}$ cannot be observed. However, we can demonstrate the low pass filtering of laser cooled Ca^{+} isotopes utilizing the dependence on the dc voltage.

3.3. Numerical simulations

We performed numerical simulations with the SIMION software (Scientific Instrument Services) to analyze the results of the experiments. The actual geometry of our trap electrodes was used and the electric field was calculated by finite difference method in this simulation. First of all, we checked the differences between the single ion flights and the 100 ion cloud. As a series of simulated results, the effects of the space charge effect and the Coulomb repulsions with the function of the SIMION showed small change of the ion trajectory. However, the calculation time of the 100 ion cloud is longer than that of 100 single ions. For that reason, we used single ion flights to observe the dependence on the trapping dc voltage. To save the computation resource we employed mirror symmetry condition to the axial direction and a trajectory of a single ion was calculated hundred times to obtain averaged results. The velocity of initial injected ions was based on a Maxwell Boltzmann distribution in three dimensions. We assumed 10 K as the initial temperature of trapped ions from the spectra of trapped Ca^{+} ions. In our calculation the dependence on the initial ion position was found to be small. So the initial ions are placed at the trap central axis. The real trapping time in the experiments was long, but in our simulation the maximum flight time was limited to 10 ms, which corresponds to 10,000 rf periods, because of computer power. The mass number and dc voltage are utilized as calculation parameters in these calculations. We set the rf voltage to $V_{rf} = 150, 200$, and 235 V for each parameter. Here, we focus the relationship between the trapping dc voltage and the trapping efficiency at $V_{rf} = 150$ V in Fig. 5. The ratio corresponds to the number of trapped ions. We also calculated and checked other conditions. The tendencies of the simulation results are similar to those of the experimental results. In addition, the calculation result shows the clear boundary of the dc voltages because the electrode symmetry of calculation is better than that of experiment.

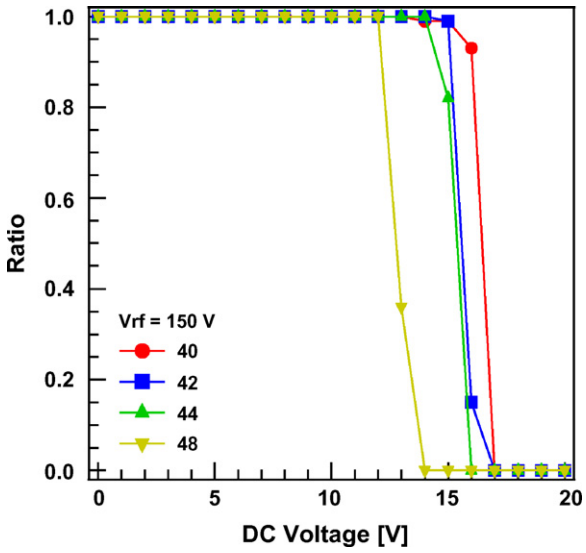

Fig. 5. Simulation results with SIMION for $V_{rf} = 150$ V. The maximum trapping time is 10 ms because of the long calculation time. We found similar tendencies as in the experiment. In addition the boundary of the dc voltages of simulation is clearer than that of experiment.

3.4. Nonlinear resonance

From measurement of the dependences on the rf and dc voltage, we found the drastic decreasing of the trapping efficiencies for each isotope even within stable region of the Mathieu diagram.

The trapped ions change the trapping potential. In addition, the finite electrode structure of a real trap, misalignments or modifications of the electrodes, and other effects may generate non-quadratic contributions to the trap potential. They can be summarized by an expansion of the trap potential with multiple components. In cylindrical coordinates it is described by

$$\Phi_{real}(r, \phi, t) = (U_{dc} + V_{rf} \cos \Omega t) \sum_{k=0}^{\infty} c_k \left(\frac{r}{r_0}\right)^k \cos k\phi, \quad (4)$$

where c_k shows the strength of the perturbing potential of order k [33,34]. For $k = 2$, we have the ideal quadrupole potential. In principle, a contribution of the order k can cause nonlinear resonances of the orders $N = k, k-2, k-4, \ldots$. All terms with odd k vanish in Eq. (4), because of the mirror symmetry with respect to the trap midplane [33,34]. However, if the construction is not perfect there will be odd k terms as well as even. Furthermore, we should consider the effect of the end cap electrodes because of the axial confinement.

Higher order terms in the trapping potential influence the motion of trapped ions. If the secular frequencies ω_x, ω_y, and ω_z in the pseudopotential fulfill the condition [33,34].

$$n_x\omega_x + n_y\omega_y = \Omega - k_z\omega_z, \quad k_z = 0, 1, 2, \ldots, |n_x| + |n_y| = N, \quad (5)$$

where n_x, n_y are integers, a nonlinear resonance of N-th order is generated and the motion of the ion is unstable inside the stable region of the Mathieu diagram. The secular frequencies are described by [33].

$$\omega_x \simeq \frac{\Omega}{2}\sqrt{\frac{q^2}{2} + a_x - \frac{1}{2}a_z}, \quad (6)$$

$$\omega_y \simeq \frac{\Omega}{2}\sqrt{\frac{q^2}{2} + a_y - \frac{1}{2}a_z}, \quad (7)$$

$$\omega_z = \frac{\Omega}{2}\sqrt{a_z} = \sqrt{\frac{2\kappa e V_{cap}}{m z_0^2}}, \quad (8)$$

with $a_z = 8\kappa e V_{cap}/m z_0^2 \Omega^2$ where κ is a geometrical parameter determined by the trap geometry. For our electrode configuration we obtain $\kappa = 0.09$.

To analyze our experimental observations we calculated the a and q values, where the nonlinear resonances were observed, and plotted them on the stability diagram. Furthermore we added the theoretical expected values for $N = 3$ (hexapole) $\sim$ 10 (icosapole) as eye guides: the lines for $k_z = 0$ and $n_x = 0$ or $n_y = 0$ are plotted (Fig. 6). When the dc voltage scanning, we fixed the rf voltage. So observed nonlinear resonances of each isotope are not overlapped, while in the case of rf scanning observed nonlinear resonances

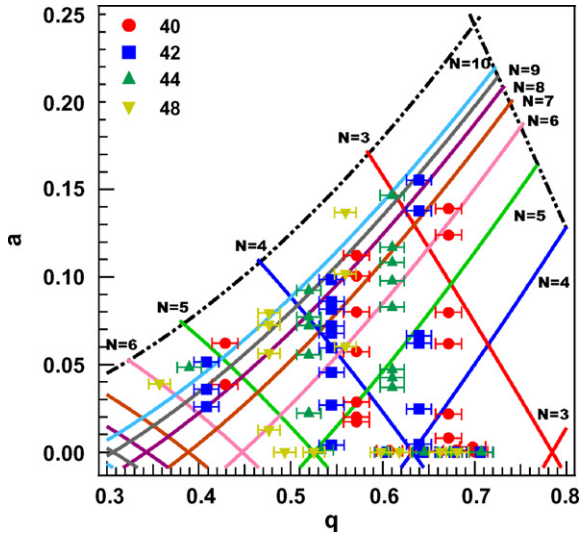

Fig. 6. Nonlinear resonances of the experimental observations. The theoretical expectations for $N = 3$ (hexapole) ~ 10 (icosapole) as eye guides: the lines for $k_z = 0$ and $n_x = 0$ or $n_y = 0$ are plotted. The unstable operating points follow closely the calculated lines, which include odd number lines. Thus, we can find the imperfection of our trapping system.

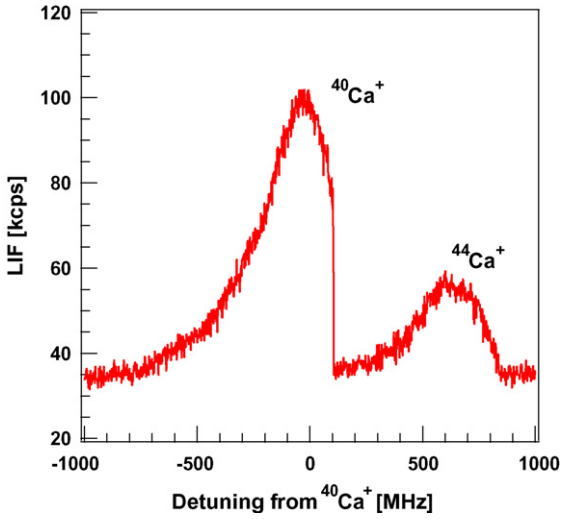

Fig. 7. Simultaneous observation of the spectra of $^{40}Ca^+$ and $^{44}Ca^+$. The frequency of the 397 nm laser is scanned from −1000 MHz to +1000 MHz from the resonance of $^{40}Ca^+$, while the frequencies of two 866 nm laser are set to the resonances of both isotopes. The 866 nm laser for $^{40}Ca^+$ is turned off when the frequency of 397 nm gets slightly above the resonance to avoid laser heating. The frequencies of both peaks correspond to the respective isotope shifts.

are overlapped considering the error bars. The unstable operating points follow closely the calculated lines, which include odd N number lines. Thus, we can find the imperfection of our trap electrode alignment. From our limited results we cannot assign N, n_x, n_y, and k_z. Drakoudis et al. observed nonlinear resonances of a few ions in the range a from −0.08 to 0.08, q from 0.35 to 0.7, where the resonances sparsely occur [33]. In order to make an accurate comparison between the experimental observations and theoretical calculations, we should observe the nonlinear resonances for a fixed number of trapped single isotope ions with high resolution scanning and calculate the complex model considering the same number of trapped ions, the interaction between ions, and so on.

4. Isotope separation of trapped Ca^+ ions

4.1. Demonstrating the high pass filter function

We investigated the prospect of utilizing the high pass filter function for $^{40}Ca^+$ and $^{44}Ca^+$ utilizing the dependence on the rf voltage. First we loaded Ca^+ ions. In order to laser-cool $^{40}Ca^+$ and $^{44}Ca^+$ simultaneously, the frequency of the 397 nm laser is set below the resonance of $^{40}Ca^+$ and the frequencies of the two 866 nm lasers are set on the resonances of $^{40}Ca^+$ and $^{44}Ca^+$, respectively. We can observe the LIF spectra of both isotopes shown in Fig. 7 by scanning the frequency of 397 nm from −1000 MHz to +1000 MHz relative to the resonance of $^{40}Ca^+$. The 866 nm laser for $^{40}Ca^+$ is turned off when the frequency of 397 nm laser gets slightly above the resonance of $^{40}Ca^+$, to avoid the laser heating effect.

Thus we experimentally demonstrated the high pass filtering function by increasing the rf voltage. Fig. 8 shows the temporal profiles of the LIF, the piezo transducer (PZT) voltage of the 397 nm ECDL, and the rf voltage. The frequency of the 397 nm laser, which corresponds to the PZT voltage V_{pzt} is set to the resonance of $^{40}Ca^+$ and the LIF of $^{40}Ca^+$ is maximum. To trap both isotopes of $^{40}Ca^+$ and $^{44}Ca^+$, we set the rf voltage $V_{rf} = 217.5$ V. Here, the LIF of $^{40}Ca^+$ is the main component because the frequency of the 397 nm is set to the resonance of $^{40}Ca^+$. Therefore, we can consider the decrease of the LIF as the reduction of the number of $^{40}Ca^+$. We found that the LIF decreases to the background level, when increasing V_{rf} to 240 V. Furthermore, we can observe $^{44}Ca^+$ in the trap when the 397 nm laser reaches the resonance for $^{44}Ca^+$. This demonstrates the high pass filtering of laser cooled Ca^+ isotopes. We suggest that our method is simpler than the laser heating method because we only control the rf voltage while laser heating requires to control several lasers at the same time [13].

After the reduction of lighter isotopes, we can observe the heavier isotopes by directly and sympathetically cooling the ions. From

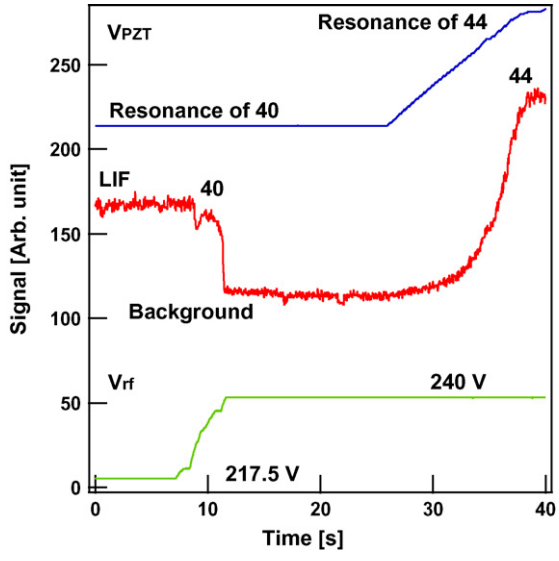

Fig. 8. Demonstration of the high pass filter function. First, $^{40}Ca^+$ and $^{44}Ca^+$ are trapped and laser-cooled. The frequency of the 397 nm laser is optimized to maximize the LIF of $^{40}Ca^+$. The 866 nm lasers for both isotopes are always on. We can observe the decrease of the LIF of $^{40}Ca^+$ to the background with the increase of the rf voltage from $V_{rf} = 217.5$ V to $V_{rf} = 240$ V. After filtering $^{40}Ca^+$, we can observe $^{44}Ca^+$ scanning the frequency of the 397 nm laser. Here, the frequency of the 397 nm laser corresponds to the piezo transducer voltage, V_{PZT}.

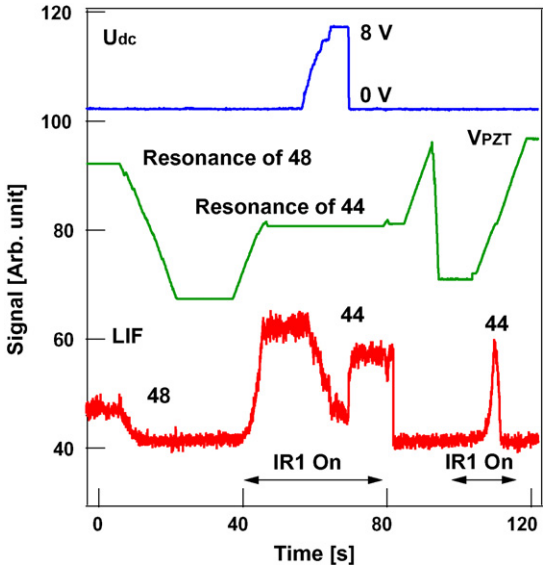

Fig. 9. Demonstration of the low pass filter function. First $^{44}Ca^+$ and $^{48}Ca^+$ are trapped and laser cooled. The rf voltage is set $V_{rf} = 150$ V in order to utilize the low pass filter function. Here, IR1 and IR2 indicate the 866 nm lasers for $^{44}Ca^+$ and $^{48}Ca^+$, respectively. IR2 is always turned on. First, we set the frequency of 397 nm to the resonance of $^{48}Ca^+$, and we can observe the LIF of $^{48}Ca^+$, where IR1 is turned off. Then, we could observe the LIF of $^{44}Ca^+$ with the IR1 radiation. From here, we increased the dc voltage U_{dc} to ~ 8 V, and reset to zero. After that, we could reduce $^{48}Ca^+$ and observe $^{44}Ca^+$. Here, the frequency of the 397 nm laser corresponds to V_{PZT}.

cooling spectra we can observe the reduction of $^{40}Ca^+$ and $^{42}Ca^+$ and the existence of $^{44}Ca^+$ and $^{48}Ca^+$.

4.2. Demonstrating the low pass filter function

To exclude the heaviest $^{48}Ca^+$ isotope after high pass filtering, we investigated the possibility of using the low pass filter function for $V_{rf} = 150$ V. Fig. 9 shows the temporal profiles of the LIF, the PZT voltage of the 397 nm ECDL, and the dc voltage. Here, IR1 and IR2 indicate the 866 nm lasers for $^{44}Ca^+$ and $^{48}Ca^+$, respectively, and both frequencies are set to the resonances. In Fig. 9, IR2 is always turned on. First, we observed LIF from $^{48}Ca^+$ after preparing $^{44}Ca^+$ and $^{48}Ca^+$. Then the frequency of the 397 nm laser is set −1000 MHz from the resonance of $^{44}Ca^+$ and IR1 is turned on. The cooling and repumping laser frequencies are chosen in order to maximize the LIF. After that, we gradually increased the dc voltage U_{dc} to ~ 8 V, at which $^{48}Ca^+$ ions are expelled from the trapping region, and decreased U_{dc} to 0 V. Here, we can see the change of LIF of $^{44}Ca^+$. Because of the applied dc voltage, not only $^{48}Ca^+$ but also $^{44}Ca^+$ can be heated and lost from the trapping region. In addition, trapped ions are moved by the changing of trapping potential and effective laser cooling may not be performed. After the eliminating of $^{48}Ca^+$ we can also find the recovery of LIF of $^{44}Ca^+$ because of laser cooling. To check the elimination of $^{48}Ca^+$, we scanned the frequency of the 397 nm laser and the LIF of $^{48}Ca^+$ disappeared at the resonance. However we could observe the $^{44}Ca^+$ with IR1. This shows that we demonstrated the low pass filtering of laser-cooled Ca^+ isotope and the selective loading of the isotope of interest by manipulating V_{rf} and U_{dc}.

We investigated the direct trapping of a particular isotope with the functions of high and low pass filter. However, we could not realize direct trapping of the isotope of interest. This is because, when the dc voltage is applied, the ablated electrons cannot shunt the trapping potential. Thus the ablated Ca^+ ions cannot enter the trap region. This is in good agreement with the SIMION simulation.

5. Conclusion

We investigated the dependences of the trapping ratios of the Ca^+ isotopes on the rf and dc voltages with existences of several isotopes. Furthermore, we demonstrated for the first time the isotope manipulation of laser-cooled Ca^+ ions using the mass selectivity of the linear Paul trap. In addition, we observed the nonlinear resonances of each isotope in the stable region of the Mathieu diagram.

As the next step towards the analysis of $^{41}Ca^+$, we should realize the observation of the odd isotopes and the selective loading of the ultra trace isotope. Thus, we are planning to develop new experimental devices, such as hyperfine repumping system and selective loading system to observe the odd isotope of $^{43}Ca^+$ and the rarest stable isotope of $^{46}Ca^+$. Finally, with these combined methods we will approach to the detection of $^{41}Ca^+$.

Acknowledgments

The authors acknowledge the valuable suggestions and comments of two reviewers. We also thank Drs. K. Okada, M. Miyabe, Y. Kaneta, M. Todoriki and I. Buluta for several supports. The first author would like to acknowledge the support of the Japan Society for Promotion Science, by a Grant-in-Aid for JSPS fellows.

References

[1] E.G.H.M. van den Heuvel, G. Schaafsma, T. Muys, W. van Dokkum, Am. J. Clin. Nutr. 67 (1998) 445.
[2] K.Y. Patterson, C. Veillon, A.D. Hill, P.B. Moser-Veillon, T.C. O'Haver, J. Anal. At. Spectrom. 14 (1999) 1673.
[3] L. Halicz, A. Galy, N.S. Belshaw, R.K. O'Nions, J. Anal. At. Spectrom. 14 (1999) 1835.
[4] D. Elmore, M.H. Bhattacharyya, N. Sacco-Gibson, D.P. Peterson, Nucl. Instrum. Methods Phys. Res., Sect. B 52 (1990) 531.
[5] W. Henning, W.A. Bell, P.J. Billquist, B.G. Glagola, W. Kutschera, Z. Liu, H.F. Lucas, M. Paul, K.E. Rehm, J.L. Yntema, Science 236 (1987) 725.
[6] D. Fink, J. Klein, R. Middleton, Nucl. Instrum. Methods Phys. Res., Sect. B 52 (1990) 572.
[7] K. Nishiizumi, M.W. Caffee, D.J. DePaolo, Nucl. Instrum. Methods Phys. Res., Sect. B 172 (2000) 399.
[8] P. Müller, B.A. Bushaw, K. Blaum, S. Diel, C. Geppert, A. Nahler, N. Trautmann, W. Noertershaeuser, K. Wendt, Fresenius J. Anal. Chem. 370 (2001) 508.
[9] I.D. Moore, K. Bailey, J. Greene, Z.-T. Lu, P. Müller, T.P. O'Connor, Ch. Geppert, K.D.A. Wendt, L. Young, Phys. Rev. Lett. 92 (2004) 153002.
[10] Ch. Geppert, P. Müller, K. Wendt, Ch. Schnabel, H.-A. Synal, U. Herpers, S. Merchel, Nucl. Instrum. Methods Phys. Res., Sect. B 229 (2005) 519.
[11] D.J. Wineland, J.C. Bergquist, J.J. Bollinger, W.M. Itano, D.J. Heinzen, S.L. Gilbert, C.H. Manney, M.G. Raizen, IEEE Trans. Ultrason. Ferroelectr. Freq. Control 37 (1990) 515.
[12] J.I. Cirac, P. Zoller, Phys. Rev. Lett. 74 (1995) 4091.
[13] K. Toyoda, H. Kataoka, Y. Kai, A. Miura, M. Watanabe, S. Urabe, Appl. Phys. B 72 (2001) 327.
[14] S. Hasegawa, L. Matsuoka, Y. Fukushima, H. Osaki, Y. Hashimoto, J. Nucl. Sci. Technol. 43 (2006) 300.
[15] D.J. Berkeland, Rev. Sci. Instrum. 73 (2002) 2856.
[16] Y. Hashimoto, L. Matsuoka, D. Nagamoto, S. Hasegawa, Spectrochim. Acta B 63 (2008) 645.
[17] K. Sugiyama, J. Yoda, IEEE Trans. Instrum. Meas. 44 (1995) 140.
[18] R. Alheit, K. Enders, G. Werth, Appl. Phys. B 62 (1996) 511.
[19] W. Alt, V. Schmidt, T. Nakamura, P. Seibert, X. Chu, G. Werth, J. Phys. B: At. Mol. Opt. Phys. 30 (1997) L677.
[20] T. Hasegawa, T. Shimizu, Appl. Phys. B 70 (2000) 867.
[21] U. Tanaka, H. Imajo, K. Hayasaka, R. Ohmukai, M. Watanabe, S. Urabe, Opt. Lett. 22 (1997) 1353.
[22] N. Kjaergaard, L. Hornekaer, A.M. Thommesen, Z. Videsen, M. Drewsen, Appl. Phys. B 71 (2000) 207.
[23] S. Gulde, D. Rotter, P. Barton, F. Schmidt-Kaler, R. Blatt, W. Hogervorst, Appl. Phys. B 73 (2001) 861.
[24] D.M. Lucas, A. Ramos, J.P. Home, M.J. McDonnell, S. Nakayama, J.-P. Stacey, S.C. Webster, D.N. Stacey, A.M. Steane, Phys. Rev. A 69 (2004) 012711.
[25] U. Tanaka, H. Matsunishi, I. Morita, S. Urabe, Appl. Phys. B 81 (2005) 795.
[26] U. Tanaka, I. Morita, S. Urabe, Appl. Phys. B 89 (2007) 195.
[27] W. Paul, Rev. Mod. Phys. 62 (1990) 531.
[28] F. Diedrech, E. Peik, J.M. Chen, W. Quint, H. Walther, Phys. Rev. Lett. 59 (1987) 2931.

[29] Y. Hashimoto, L. Matsuoka, H. Osaki, Y. Fukushima, S. Hasegawa, Jpn. J. Appl. Phys. 45 (2006) 7108.
[30] A.M. Martensson-Pendrill, A. Ynnerman, H. Warston, L. Vermeeren, R.E. Silverans, A. Klein, R. Neugart, C. Schulz, P. Lievens, Phys. Rev. A 45 (1992) 4675.
[31] W. Nörtershäuser, K. Blaum, K. Icker, P. Müller, A. Schmitt, K. Wendt, B. Wiche, Eur. Phys. J. D 2 (1998) 33.
[32] U. Tanaka, S. Urabe, M. Watanabe, Appl. Phys. B 78 (2004) 43.
[33] A. Drakoudis, M. Söllner, G. Werth, Int. J. Mass Spectrom. 252 (2006) 61.
[34] Y. Wang, J. Franzen, K.P. Wanczek, Int. J. Mass Spectrom. Ion Processes 124 (1993) 125.